Neuro-Oncology Advances
2(1), 1–12, 2020 | doi:10.1093/noajnl/vdaa083 | Advance Access date 4 July 2020

Multiomics profiling of paired primary and recurrent glioblastoma patient tissues

Lennard J. M. Dekker†, Nynke M. Kannegieter†, Femke Haerkens, Emma Toth, Johan M. Kros, Dag Are Steenhoff Hov, Julien Fillebeen, Lars Verschuren, Sieger Leenstra, Anna Ressa, and Theo M. Luider

Department of Neurology, Erasmus University Medical Centre Rotterdam, Rotterdam, The Netherlands (L.J.M.D., E.T., T.M.L.); Pepscope BV, Utrecht, The Netherlands (N.M.K., F.H., A.R.); Department of Pathology, Erasmus University Medical Centre Rotterdam, Rotterdam, The Netherlands (J.M.K.); PubGene AS, Oslo, Norway (D.A.S.H., J.F.); Department of Microbiology and Systems Biology, The Netherlands Organization for Applied Scientific Research (TNO), Zeist, The Netherlands (L.V.); Department of Neurosurgery, Erasmus University Medical Centre Rotterdam, Rotterdam, The Netherlands (S.L.)

†*These authors contributed equally to this work.*

Corresponding Authors: Theo M. Luider, PhD, Department of Neurology, Erasmus University Medical Centre Rotterdam, P.O. Box 2040, 3000 CA Rotterdam, The Netherlands (t.luider@erasmusmc.nl); Anna Ressa, PhD, Pepscope BV, Padualaan 8, 3584 CH Utrecht, The Netherlands (anna@pepscope.com).

Abstract

Background. Despite maximal therapy with surgery, chemotherapy, and radiotherapy, glioblastoma (GBM) patients have a median survival of only 15 months. Almost all patients inevitably experience symptomatic tumor recurrence. A hallmark of this tumor type is the large heterogeneity between patients and within tumors itself which relates to the failure of standardized tumor treatment. In this study, tissue samples of paired primary and recurrent GBM tumors were investigated to identify individual factors related to tumor progression.

Methods. Paired primary and recurrent GBM tumor tissues from 8 patients were investigated with a multiomics approach using transcriptomics, proteomics, and phosphoproteomics.

Results. In the studied patient cohort, large variations between and within patients are observed for all omics analyses. A few pathways affected at the different omics levels partly overlapped if patients are analyzed at the individual level, such as synaptogenesis (containing the SNARE complex) and cholesterol metabolism. Phosphoproteomics revealed increased STMN1(S38) phosphorylation as part of ERBB4 signaling. A pathway tool has been developed to visualize and compare different omics datasets per patient and showed potential therapeutic drugs, such as abobotulinumtoxinA (synaptogenesis) and afatinib (ERBB4 signaling). Afatinib is currently in clinical trials for GBM.

Conclusions. A large variation on all omics levels exists between and within GBM patients. Therefore, it will be rather unlikely to find a drug treatment that would fit all patients. Instead, a multiomics approach offers the potential to identify affected pathways on the individual patient level and select treatment options.

Key Points

- Large heterogeneity of GBM tumors is confirmed by multiomics approach.
- Multiomics analyses give insights on tumor progression at the individual level.
- Based on individual pathway analyses, potential treatment options can be selected.

Importance of the Study

In GBM patients, the tumor almost always recurs after current standard therapy. Since there is no adequate therapy for tumor recurrence survival is very poor. In this study, we investigated if a multiomics comparison of paired primary and recurrent GBM tissue samples can increase the understanding of tumor progression at the individual patient level.

Glioblastoma (GBM) is the most common and malignant primary brain tumor with an overall patient survival of less than 15 months.[1] Current standardized GBM therapy consists of maximal tumor bulk resection and subsequent radiotherapy with concomitant temozolomide (TMZ) treatment.[2] The prognosis of GBM has improved very little since a decade ago when TMZ was added to postoperative fractionated radiotherapy. GBM recurs in nearly all patients and is often resistant to initial therapy,[3] thereby limiting the median survival to only 5–7 months upon recurrence and a second round of therapy.

No effective treatment for GBM has been developed thus far, despite the large number of clinical trials that have been performed.[4] Problems experienced in explored treatments arise in part from the inaccessibility of the tumor. Diffusion of GBM into surrounding tissue makes total surgical resection strenuous, while the blood–brain barrier hinders the delivery of most drugs.[1] Another cause for treatment failure is the resistance of subclones within the tumor and development of acquired resistance in other subclones.[5] Well-known mechanisms of resistance are the high expression and activity of DNA repair enzyme O^6-methylguanine DNA methyltransferase (*MGMT*), epidermal growth factor receptor (*EGFR*), murine double minute (*MDM2*), inactivating mutations of (*TP53*), *PTEN*, and *MMR* genes.[6] Although the related proteins have been exploited as therapeutic targets, none of the developed treatments has shown efficacy.[7]

The poor outcome of clinical trials can to a great extent be explained by bypassing the targeted signaling pathways via coactivation of complementary pathways, thereby decreasing the effect of the administered drug.[8,9] The highly heterogeneous nature of GBM, lack of proper patient stratification in clinical trials, and the presence of GBM stem cells, which are thought to have innate TMZ resistance,[10] are other causes of drug treatment failure. The highly heterogeneous nature of GBM is reflected in large differences in signaling pathway expression and activation between tumors. Thus, recurrent GBM biology in individual cases must be further studied to obtain valuable information on how involved pathways are regulated and altered after standard treatment protocols. In fact, this approach is an extension of recent insights that clinical trials for GBM need to be designed in a different way. Examples of these new designed clinical trials are adaptive studies with basket and umbrella designs aimed at optimizing the biomarker–drug codevelopment process.[7,11]

In a study of Wang et al.,[12] a relatively large series of primary and recurrent GBM tumors were investigated at the transcriptomics level. On these samples, the transcriptome clusters, classical (CL), mesenchymal (MES), and proneural (PN) introduced by Verhaak et al.,[13] were applied. This study showed that in 55% of the investigated cases the transcriptome cluster between the primary and recurrent tumor is retained, indicating that the variation between paired primary and recurrent tumors is probably lower compared to unpaired tumors. This has also been demonstrated for the *EGFR* amplification which is retained in 84% of the cases between primary and recurrent GBM[14] and in 80% of the cases the molecular events are stable.[15] These studies support the concept of studying tumor progression and recurrence on the individual level. The limited availability of paired primary and recurrent GBM samples is a complicating factor for such studies. However, large-scale multicenter consortia like GLASS have collected larger sample cohorts of paired primary and recurrent glioma samples,[16] resulting in a number of molecular studies.

In the present study, the pathophysiological changes underlying tumor recurrence and progression were investigated. This was achieved by identifying the changed expression of canonical signaling pathways through a multiomics workflow. The emergence of numerous omics technologies has made it possible to resolve the molecular signatures, correlation, and crosstalk of different layers of biological information.[17,18] In recent years, the complementary possibilities of different omics technologies have been shown,[19] but until now, no multiomics studies have been published on paired primary and recurrent GBM. Especially, proteomics and phosphoproteomics have shown to give additional information about signaling.[20–24]

Materials and Methods

GBM Patients

Eight patients with histologically confirmed GBM who underwent surgery of primary and recurrent disease at Erasmus Medical Center (Rotterdam, the Netherlands) were retrospectively studied (Table 1). All patients received a similar scheme of first-line treatment, maximal surgical resection followed by radiotherapy with concomitant and adjuvant TMZ-based chemotherapy.[25] The use of patient material for research was approved by the Institutional Review Board of the Erasmus MC, Rotterdam, the Netherlands (MEC 221.520/2002/262, approval date July 22, 2003; MEC-2005-057, approval date February 14, 2005). All patients gave written informed consent for the research use of the tissue specimens.

Table 1. Patient Characteristics

	Study population ($n = 8$ pairs of primary and recurrent brain tumors)
Age (years)	51 (28–56)
Gender (male/female)	4 (50%)/4 (50%)
OS (months)	27 (10–45)
PFS (months)	19.5 (6–41)
Tumor location	
Frontal	0
Temporal	3
Parietal	2
Occipital	0
Multiple	2
NA	1
Tumor pathology	
GBM	8
Treatment postoperative	
RT +TMZ	8
Treatment after disease progression	
Surgery	5
Surgery + Lomustine	3
Tumor content of samples	
Primary 60%–70% tumor	6
Primary 50% tumor	2
Recurrent 60%–70% tumor	7
Recurrent 40% tumor	1

Tissue Sampling

GBM fresh-frozen tissue samples from all patients, from both primary and recurrent surgery, were aliquoted in 2 Eppendorf for (phospho)proteomics and transcriptomics analysis. For each aliquot, tissue sections of 8 µm thickness were sliced with a Cryostat (Thermo Fischer Scientific) and immediately stored at –80°C. In addition, tissue sections of 4 µm thickness were processed for standard H&E staining to assess the presence of tumor cells equal to at least 40%.

Sample Preparation and Mass Spectrometry

GBM fresh-frozen tissue sections were prewashed, lysed, and then sonicated. After measuring the total protein concentration, proteins were reduced, alkylated, and subsequently tryptic digested overnight. Peptides were desalted, and subsequently, the total peptide concentration was measured for each sample. Desalted peptides were labeled with tandem mass tag (TMT) 10-plex labeling reagents and a check for labeling efficiency and mixing ratio across channels were performed. Samples were then combined in an equal ratio, desalted, and subjected to phospho-enrichment on FeNTA tips. The flow-through of the enrichment was fractionated off-line by basic pH reverse-phase high performance liquid chromatography. Both peptides and phosphopeptides were processed by an Liquid chromatography tandem mass spectrometry method using an Ultimate 3000RS LC system (Thermo Fisher Scientific) operating in nano-flow coupled to a Q-Exactive HF mass spectrometer (Thermo Fisher Scientific). Further details and experimental parameters are outlined in Supplementary Methods.

Transcriptomics Analysis

GBM fresh-frozen tissue sections were processed by the MAD Dutch Genomics Service & Support Provider (Amsterdam, the Netherlands) for transcriptomics analysis. Further details are outlined in Supplementary Methods.

Proteomics and Phosphoproteomics Data Analysis

All mass spectrometry RAW data files were analyzed by MaxQuant (version 1.6.5.0, www.coxdocs.org) using the integrated Andromeda search engine and Swiss-Prot Homo sapiens database (20 417 entries, 03_2019). Data analysis of the generated proteomics and phosphoproteomics datasets was performed using R-package Proteus,[26] Perseus (version 1.6.5.0, www.coxdocs.org), GraphPad Prism (version 8.2.1), Microsoft Excel, and Ingenuity Pathway Analysis software (IPA, Qiagen). TMT reporter intensity values were used to perform statistical analysis. For a complete proteomics and phosphoproteomics data analysis workflow, see Supplementary Methods.

Signaling Pathway Analysis

IPA was used to compare the pathways on the individual patient level. In addition, visualization of different patient data types was performed with the bioinformatic pathway tool provided by PubGene (www.pubgene.com). For more details about the signaling pathway analysis, see Supplementary Methods.

Results

Transcriptomics data of paired primary and recurrent samples, collected from 8 GBM patients, were analyzed to assess the heterogeneity between patient tumors and to investigate whether the gene expression profiles defined by Wang et al.[12] could explain GBM progression in the current study cohort. Clinical information of this study cohort is summarized in Table 1. All patients were treated with TMZ and radiotherapy after surgical resection and the overall survival time ranged from 10 to 45 months. Transcriptomics analysis quantified 21 448 transcripts across all samples. Out of the 150 signature transcripts defined by Wang et al.,[12] 139 were expressed in the present transcriptomic dataset. Unsupervised clustering of these 139 transcript expression intensities was used to

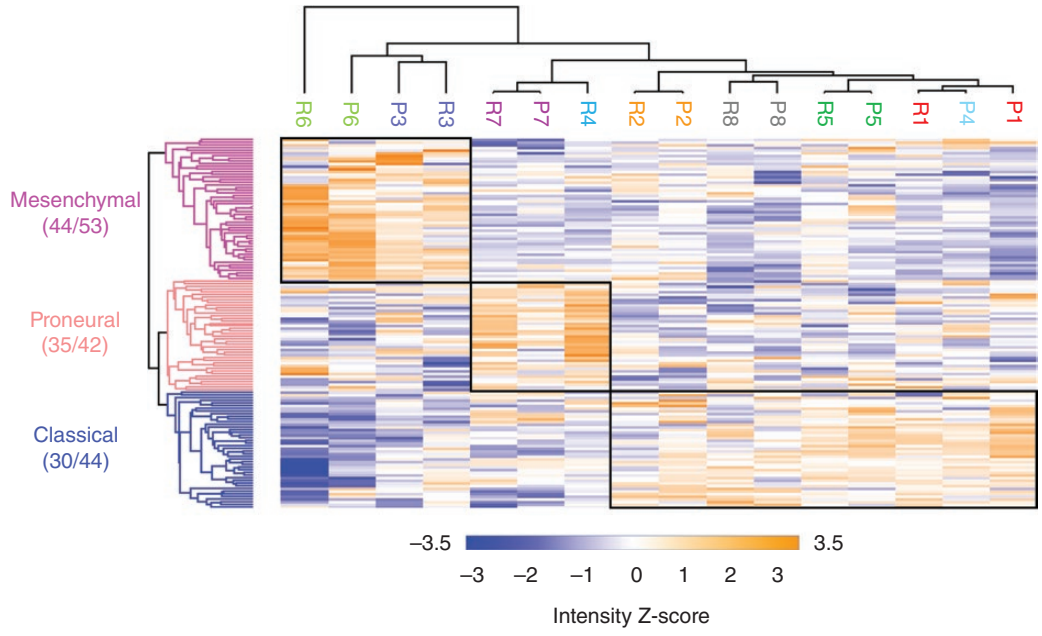

Figure 1. Identification of GBM subtypes based on transcriptomic expression. Heatmap presenting the unsupervised clustering of GBM patients based on the expression of 139 signature genes for GBM subtypes. Forty-four of 53 transcripts in the MES cluster were associated with the MES GBM subtype. PN and CL subtypes were identified with 35 and 39 transcripts, respectively.

determine the 3 GBM subtypes (Figure 1). Both primary and recurrent samples of patients 3 and 6 showed a high expression of MES transcripts (Figure 1). Primary and recurrent samples of patients 1, 2, 5, and 8 instead show high expressed transcripts belonging to the CL subtype, while patient 7 expressed a PN subtype. This division of GBM patients between subtypes confirms their high heterogeneity.

Only patient 4 switched from a CL to a PN subtype during tumor progression. In agreement with the study of Wang et al.,[12] most patients retained their subtype after tumor recurrence, suggesting that another approach is needed to explain GBM progression.

To unravel the complex nature of recurrent GBM tumors, a multiomics approach was used by combining transcriptomics with phosphoproteomics and proteomics analyses of primary and recurrent GBM samples.

In addition to the previously mentioned transcriptomics data, a total of 1470 protein groups were quantified in the GBM samples by using a TMT-labeling approach. After normalizing data for TMT-batch effects, the median coefficient of variance for primary and recurrent replicates was less than 8.4%. Principal Component Analyses (PCAs) were used as a quality control analysis for both proteomics and transcriptomics datasets. PCA of protein expression measurements revealed biological differences between primary and recurrent GBM tissue samples (Supplementary Figure 1A and B), while PCA of transcripts showed only minor differences between primary and recurrent samples and between technical replicates (Supplementary Figure 1C and D).

Next, unsupervised hierarchical clustering of primary and recurrent GBM samples was performed on both proteomics and transcriptomics datasets (Figure 2A and B). For both datasets, primary and recurrent samples did not cluster in 2 distinct groups, showing the heterogeneity between patient samples. For proteomics, also none of the recurrent samples clustered next to its primary sample (Figure 2A). In contrast to proteomics, transcript expressions of both primary and recurrent samples cluster together for the same patient (Figure 2B). This indicates that protein expression highlights biological differences between primary and recurrent GBM samples.

Differentially expressed proteins and transcripts in recurrent GBM tissues were assessed by an unpaired statistical analysis between primary and recurrent samples. For proteomics, 37 proteins were found significantly upregulated in recurrent samples, while 3 proteins were significantly downregulated (False discovery rate (FDR) cutoff = 0.05; Figure 2C). For transcriptomics, 29 downregulated and 74 upregulated transcripts were identified after applying a *P* value less than 0.05 and fold change more than 2 as a cutoff (Figure 2D). Notably, a low overlap between significantly expressed transcripts and proteins was observed, with only 2 hits identified in both datasets (ATP1B1 and INA).

In addition to proteomics and transcriptomics analysis, a phosphoproteomic analysis was performed to gain a better insight into the role of phosphorylation-driven signaling in GBM progression. A total of 681 phosphosites belonging to 356 proteins was identified and a 2-sample *t* test was performed to compare the recurrent sample

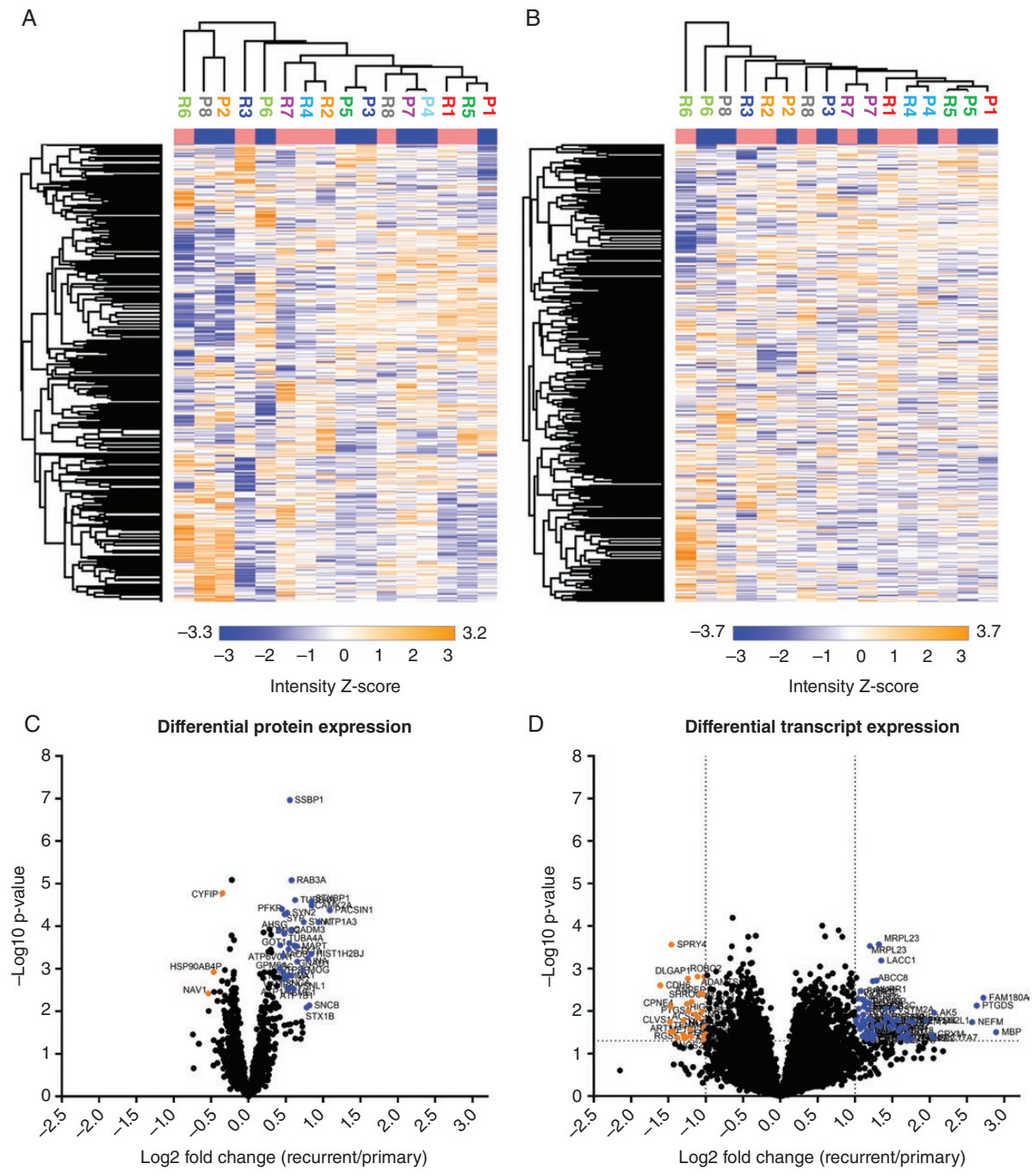

Figure 2. Proteomics and transcriptomics analysis of primary and recurrent GBM patient samples. Unsupervised hierarchical clustering of primary (blue color bar) and recurrent (salmon color bar) GBM samples based on protein expression (A) and transcript intensity (B). Volcano plots showing the significantly upregulated (blue) and significantly downregulated (orange) proteins (C) and transcripts (D) in recurrent patient samples. Significance is based on an unpaired *t* test with an FDR correction of 5%.

group versus primary samples. No phosphosites were found significantly upregulated in recurrent samples (FDR cutoff = 0.05), although RPLP1 (S104), NCAM1 (S784), STMN1(S38), and NEFM (S680/S685) expressed relatively high fold changes (log2 FC = –0.80, 0.94, 0.91, and 2.10, respectively) and relatively small *P* values ($P = 6.03 \times 10^{-5}$, 1.32×10^{-4}, 1.95×10^{-4}, and 1.55×10^{-3}, respectively; Supplementary Figure 2A).

Taken together, these findings underline the high heterogeneity between GBM patients and indicate that biological differences are present between individual primary and recurrent GBM tissue samples.

Due to the high heterogeneity among GBM patients, proteomics and transcriptomics datasets were further analyzed for each patient individually. As expected, individual multiomics analysis revealed an increased number of significant up- and downregulated hits. Proteomics significant hits increased from 40 in the total group comparison to an average of 254 per patient after individual analysis (Supplementary Figure 3A), while transcriptomics hits increased from 103 to an average of 319 per patient (Supplementary Figure 3B).

Next, all significant protein and transcript hits found in the individual multiomics analysis were selected to find a common biological signature across patients that explains GBM progression occurrence. Notably, 16 proteins and 35 transcripts were significantly changed in more than half (5 or more patients) of the recurrent patient samples as listed in Figure 3. In addition, this list showed proteins and transcripts belonging to the same family or pathway, such as the protein SYN1 (synapsin I) and transcript *SYN2* (synapsin II). Taken together, individual analysis of GBM samples revealed common up- and downregulated proteins and transcripts in recurrent samples of most, but not all GBM patients in this study cohort.

Individual patient analysis was also performed for phosphoproteomics, resulting in a significant number of up- and downregulated phosphosites with an average of 99 hits per patient sample (Supplementary Figure 2B). To find a common phosphosite that is driving GBM recurrence, a list was generated containing phosphosites with a significantly different expression in more than 5 recurrent samples (Figure 3). This list revealed 15 phosphosites representing 7 phosphoproteins being differentially expressed, including STMN1, CFL1, MAPT, KNG1, NEFM, SMARCC2, and SRSF3. Significant upregulation of STMN1(S38) in patient 3 and CFL1(S3) in patient 6 corresponded to a significant downregulation of transcripts and proteins, respectively, in the same patients (Supplementary Table 1). In addition, SMARCC2 (S302) and (S304) downregulation was associated with increased corresponding protein expression in patient 6, while no significant change was observed for proteins and transcripts corresponding to other phosphosites listed in Figure 3 (Supplementary Table 1). Altogether, this indicates that significantly changed regulation of these phosphosites was not a consequence of changed protein abundance or transcript expression.

To facilitate visualization of the integrative multiomics analysis and interpretation of proteome and transcriptome profile data, a bioinformatics pathway module was developed (Supplementary Figure 4). Within the neurotransmitter release cycle pathway (Figure 4A), protein and transcript expression of SYN1, SYN2, and RAB3A were found to be significantly changed in recurrent samples of more than half of the 8 patients (Figure 3). These proteins and transcripts have an interaction with the SNARE complex. Changed expression of SNAP25, STX1A, and VAMP2 proteins and transcripts within this complex is highly variable between recurrent patient samples. The pathway module also showed therapeutic drug options that target the SNARE complex, including abobotulinumtoxinA, incobotulinumtoxinA, onabotulinumtoxinA, and botulinum toxin type B.

The significantly changed phosphoprotein STMN1 (Figure 3) is part of the ERBB4 signaling pathway (Figure 4B). Although more than half of the patients in the study population showed a significantly increased phosphorylation of STMN1(S38), corresponding transcripts and proteins have only a limited change in expression. Therapeutic drugs targeting ERBB4 signaling include afatinib, dacomitinib, neratinib, osimertinib, and vandetanib. These drugs are currently in clinical trials (phases 1 and 2) as a treatment for GBM.

Next, a signaling pathway analysis was performed using the significantly up- and downregulated transcript and protein expressions found within each patient. Figure 5A shows the top 20 of affected signaling canonical pathways within recurrent samples of all patients based on activity *z*-scores of protein and transcript expression which indicates either an increased or decreased pathway activity in recurrent versus primary samples. The canonical pathways of synaptogenesis signaling/neurotransmitter release cycle (increased pathway activity in patients 2, 3, 4, 5, and 7; median *z*-score = 0.994), LXR/RXR activation (increased pathway activation in patients 1, 2, 3, 4, and 8; median *z*-score = 0.966), and GP6 signaling (decreased pathway activity in patients 2, 4, 5, 7, and 8; median *z*-score = –0.908) were mostly changed in recurrent GBM samples (Figure 5A). Although these 3 pathways resulted to have increased pathway activity in most patients, 3 patients showed an opposite trend. Figure 5B shows the top 20 of the affected pathways in all recurrent patient samples based on the significance of changed protein and transcript expressions instead of *z*-scores. Here, the most significantly changed pathways in recurrent samples are LXR/RXR activation (median *P* value = .0012), acute phase response signaling (median *P* value = .031), and clathrin-mediated endocytosis signaling (median *P* value = .024). In addition, synaptogenesis signaling shows a low *P* value (median *P* value = 9.78×10^{-4}; Figure 5B). However, significance levels are highly variable between patients, which is comparable with activity *z*-scores. This variability indicates heterogeneity in pathway activation between all GBM patients.

Due to this observed heterogeneity, further signaling pathway activity analysis based on a significant change in recurrent samples was performed for each patient individually (Figure 5C and D). Without sorting pathways based on combined patient results (Figure 5A and B), each patient showed a unique pathway top 5 with limited overlap between proteomics and transcriptomics (Figure 5C and D). For example, LXR/RXR activation was significantly increased in patients 1 and 4 ($P = 9.61 \times 10^{-33}$ and 8.35×10^{-9}, respectively) but decreased in patient 5 ($P = 2.38 \times 10^{-7}$). For transcriptomics, this pathway was only seen in the top 5 of patient 2 without being significant ($P = .07$). Synaptogenesis signaling was significantly increased in patients 2, 3, and 4 ($P = 1.44 \times 10^{-7}$, 2.75×10^{-4}, and 3.16×10^{-8}, respectively) for proteomics and only in patient 2 for transcriptomics ($P = 8.12 \times 10^{-3}$). In contrast, the pathway of hepatic fibrosis/stellate cell activation was only seen significantly changed in transcriptomics (6 of 8

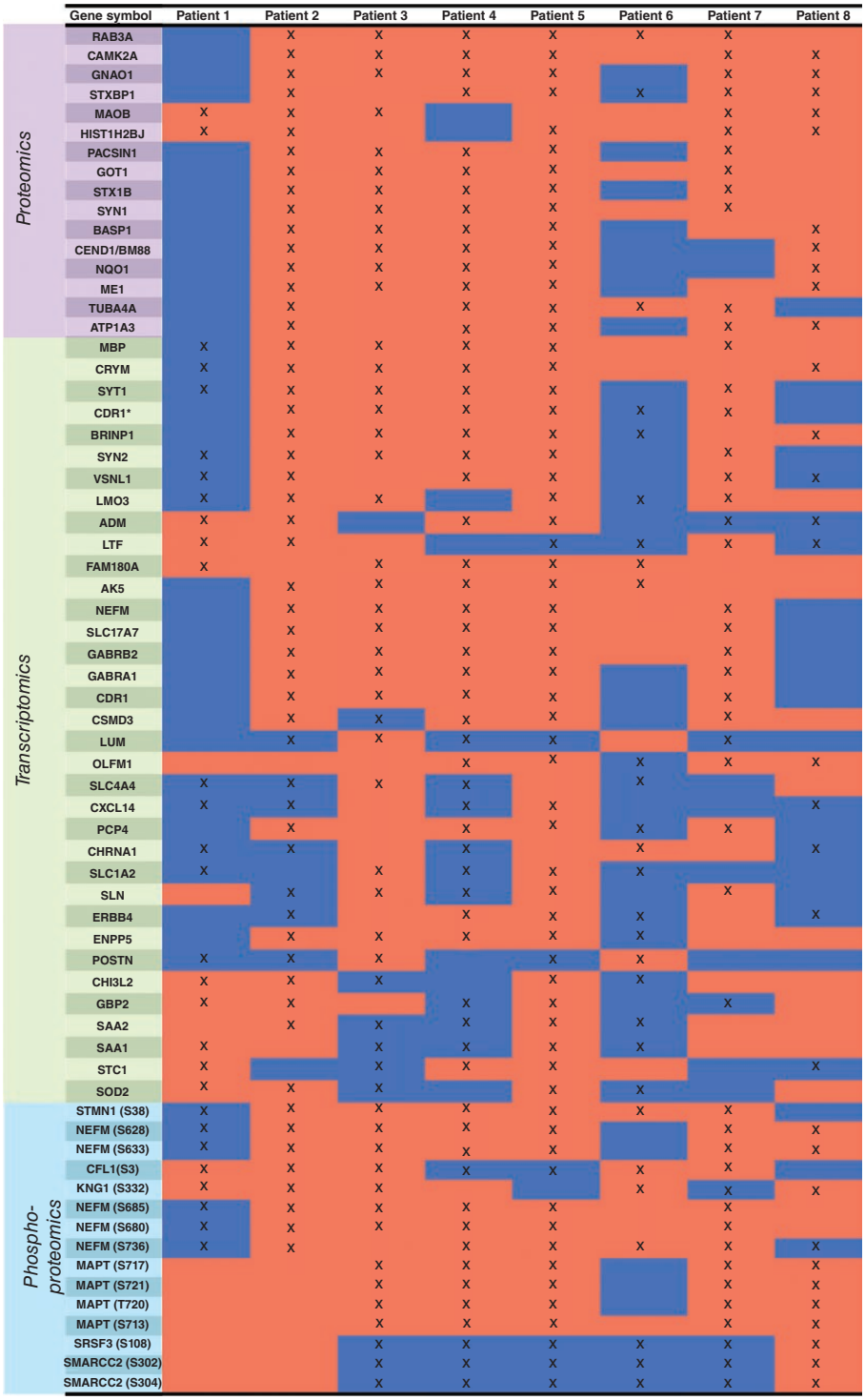

*Memczak2013 ANTISENSE, CDS, coding, downstream_end, upstream_start, UTR3, UTR5 best transcript NM_004065; CDR1 antisense RNA; CDR1 antisense RNA [Source: HGNC Symbol; Acc: HGNC: 48926]

Figure 3. List of proteins, transcripts, and phosphosites significantly changed in more than half of the study population. Significantly upregulated (orange) or downregulated (blue) proteins, transcripts, and phosphosites in the individual recurrent GBM samples are marked with "X."

patients; $P_{(p2)} = 9.68 \times 10^{-4}$, $P_{(p3)} = 2.79 \times 10^{-6}$, $P_{(p4)} = 8.60 \times 10^{-6}$, $P_{(p5)} = 3.36 \times 10^{-14}$, $P_{(p6)} = 1.51 \times 10^{-5}$, and $P_{(p7)} = 1.31 \times 10^{-2}$) and not in proteomics. These results underscore the value of individual pathways analysis to explain GBM progression. The limited overlap in individual pathway activity between transcriptomics and proteomics also shows the

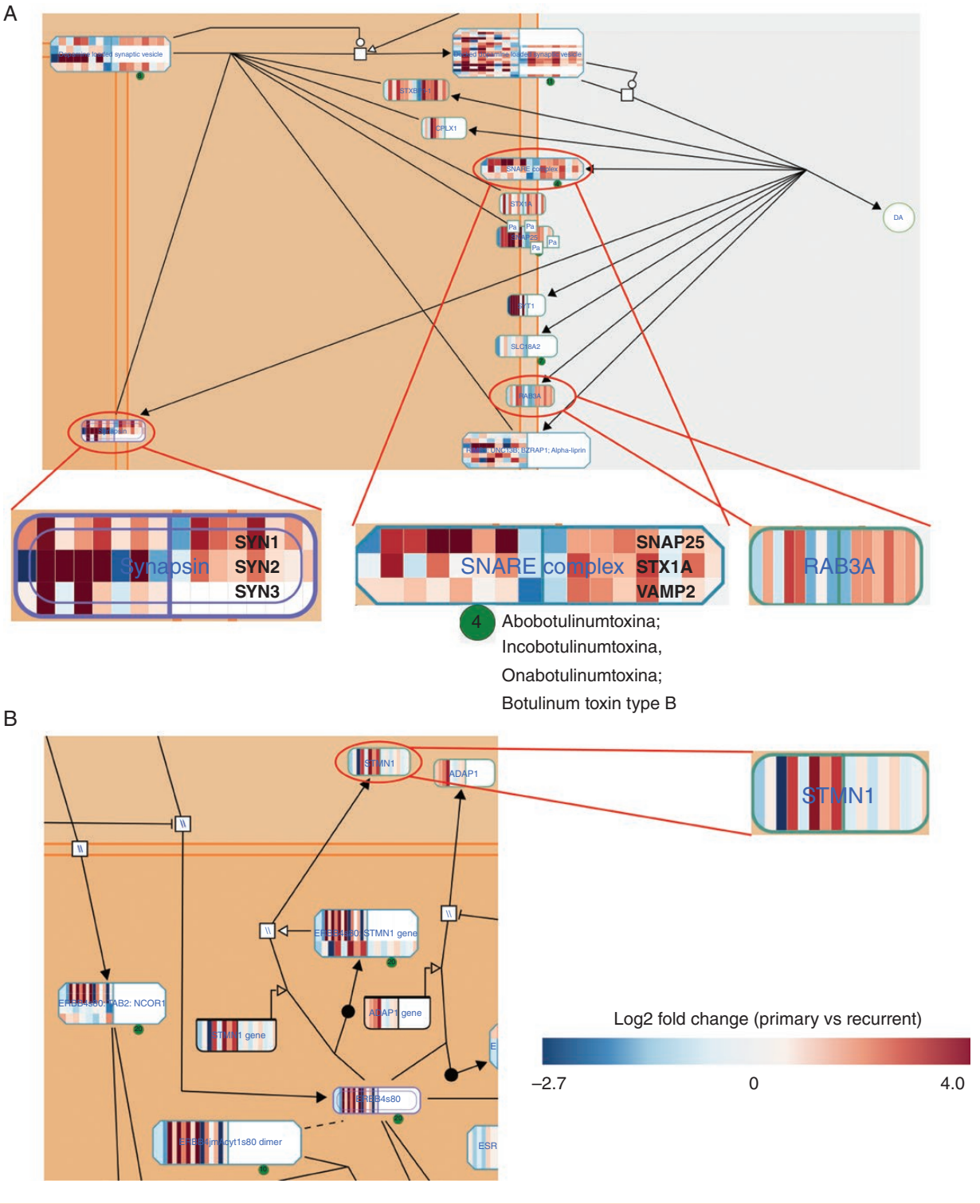

Figure 4. Signaling pathway visualization based on changed protein and transcript expression of SYN1, SYN2, SYN3, SNAP25, STX1A, RAB3A, and STMN1 in recurrent samples. (A) Expression of synapsin (SYN1, 2, and 3), RAB3A, and the SNARE complex (SNAP 25, STX1A, and VAMP2) in the neurotransmitter release cycle/synaptogenesis signaling. Four therapeutic drugs are available for targeting the SNARE complex. (B) Expression of STMN1 in ERBB4 signaling. All expressions are shown as fold changes for 8 patients in transcriptomics (left side of the box) and proteomics (right side of the box).

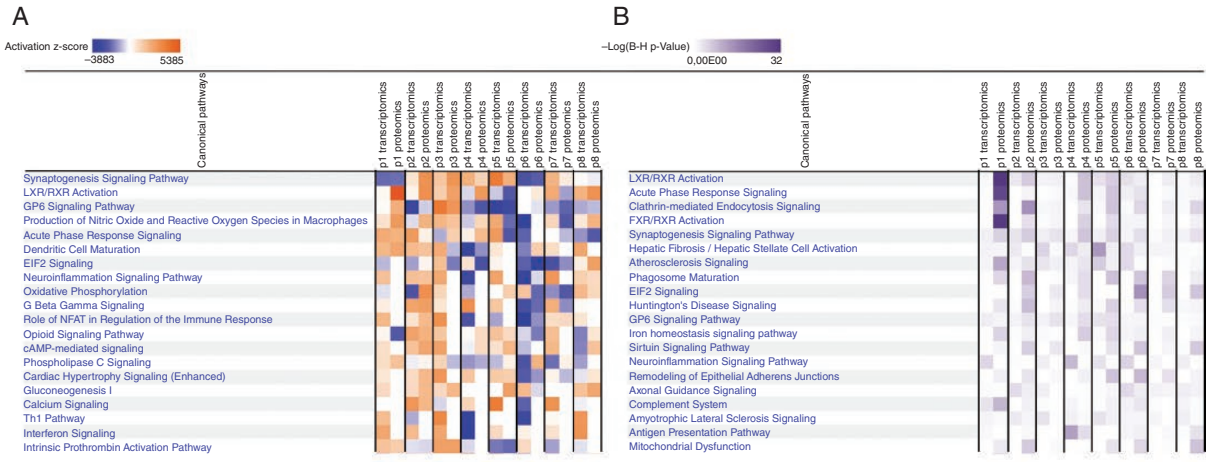

C

Patient 1	Patient 2	Patient 3	Patient 4
↑LXR/RXR Activation	Clathrin-mediated Endocytosis Signaling	↑Intrinsic Prothrombin Activation Pathway	↑LXR/RXR Activation
FXR/RXR Activation	Phagosome Maturation	Extrinsic Prothrombin Activation Pathway	↑Acute Phase Response Signaling
↑Acute Phase Response Signaling	↑Huntington's Disease Signaling	↑Synaptogenesis Signaling Pathway	↑Synaptogenesis Signaling Pathway
Clathrin-mediated Endocytosis Signaling	↑Synaptogenesis Signaling Pathway	↑GP6 Signaling Pathway	Iron homeostasis signaling pathway
Atherosclerosis Signaling	Mitochondrial Dysfunction	↓Sirtuin Signaling Pathway	FXR/RXR Activation

Patient 5	Patient 6	Patient 7	Patient 8
Phagosome Maturation	↓EIF2 Signaling	↓EIF2 Signaling	↑TCA Cycle II (Eukaryotic)
Clathrin-mediated Endocytosis Signaling	↓Remodeling of Epithelial Adherens Junctions	Phagosome Maturation	Mitochondrial Dysfunction
Remodeling of Epithelial Adherens Junctions	Phagosome Maturation	↓Huntington's Disease Signaling	↑EIF2 Signaling
↓Acute Phase Response Signaling	↑Sirtuin Signaling Pathway	Remodeling of Epithelial Adherens Junctions	↑Sirtuin Signaling Pathway
↓LXR/RXR Activation	↑RhoGDI Signaling	Epithelial AdherensJunction Signaling	↑Oxidative Phosphorylation

D

Patient 1	Patient 2	Patient 3	Patient 4
↑Neuroinflammation Signaling Pathway	Axonal Guidance Signaling	GABA Receptor Signaling	Antigen Presentation Pathway
Phagosome Formation	↑Synaptogenesis Signaling Pathway	Hepatic Fibrosis / Hepatic Stellate Cell Activation	↑Neuroinflammation Signaling Pathway
↑Complement System	↑LXR/RXR Activation	↓Estrogen-mediated S-phase Entry	↑Type I Diabetes Mellitus Signaling
Superpathway of Cholesterol Biosynthesis	Hepatic Fibrosis / Hepatic Stellate Cell Activation	nNOS Signaling in Skeletal Muscle Cells	↓Th1 Pathway
↑Glutamate Receptor Signaling	Granulocyte Adhesion and Diapedesis	↓Endocannabinoid Neuronal Synapse Pathway	Hepatic Fibrosis / Hepatic Stellate Cell Activation

Patient 5	Patient 6	Patient 7	Patient 8
Hepatic Fibrosis / Hepatic Stellate Cell Activation	↓Neuroinflammation Signaling Pathway	Cellular Effects of Sildenafil (Viagra)	Molecular Mechanisms of Cancer
Atherosclerosis Signaling	↓Sperm Motility	Axonal Guidance Signaling	Axonal Guidance Signaling
↑Opioid Signaling Pathway	Axonal Guidance Signaling	↑STAT3 Pathway	↓Neuroinflammation Signaling Pathway
↓Calcium Signaling	Hepatic Fibrosis / Hepatic Stellate Cell Activation	Hepatic Fibrosis / Hepatic Stellate Cell Activation	↓Role of Pattern Recognition Receptors in Recognition of Bacteria and Viruses
↓LPS/IL-1 Mediated Inhibition of RXR Function	Atherosclerosis Signaling	↑GPCR-Mediated Nutrient Sensing in Enteroendocrine Cells	↓Endocannabinoid Cancer inhibition Pathway

Figure 5. Significantly changed pathway activity in recurrent GBM samples, (A and B) List of canonical pathways with changed activity (A) and the corresponding significance (B) in recurrent patient samples for both proteomics and transcriptomics. (C and D) Top 5 significantly changed pathways are listed per patient for proteomics (C) and transcriptomics (D). Overlapping pathways are marked in the same color.

additional value of a multiomics approach to explain GBM progression in the individual patient.

Discussion

In this study, primary and recurrent tumor tissues from 8 GBM patients were compared to investigate the complex nature of GBM progression. Multiple omics techniques, including transcriptomics, proteomics, and phosphoproteomics, were applied.

The previously defined GBM-intrinsic gene expression subtypes called PN, CL, and MES were used to compare primary and recurrent tumors.[13,27,28] Of these subtypes, the MES subtype has been related to poor survival and the PN subtype to a more favorable outcome. Applying these GBM-intrinsic gene signatures to the transcriptomics data resulted in the clustering of patients 3 and 6 in the MES cluster.[12] This cluster has the most unfavorable survival, which is confirmed by the relatively short overall survival times of these patients. Their overall survival times were 15 months and 10 months, respectively, which were the shortest in the total study cohort. For 7 of 8 analyzed pairs of primary and recurrent GBM samples, the cluster of primary and recurrent tumors remains the same. This corresponds to data of Wang et al.[12] where clusters of primary and recurrent glioma tumors were also retained for the largest portion of analyzed samples. This indicates that transcriptomics data are probably not sufficient to explain GBM progression and that additional proteome and phosphoproteome information is required.

Unsupervised clustering of proteomics data revealed no clusters related to primary or recurrent tumors. Additionally, primary and recurrent tumors from the same patient did not cluster together. This contrasts with the clustering performed on transcriptomics data where primary and recurrent samples of a patient tend to cluster. Moreover, this shows that paired primary and recurrent GBM are in general more different on the proteomics level as compared to the transcriptomics level, indicating that proteomics data provide additional information to transcriptomics analysis. PCAs revealed that for both proteomics and transcriptomics technical variation is relatively small compared to biological variation. This reduces the possibility that differences found in the clustering of primary and recurrent transcriptomics and proteomics data are the result of technical variation. We assume that differences observed between the 2 omics technologies relate to the fact that proteome data give information about the complete protein buildup of the tumor. In contrast, transcriptomics data give a snapshot of protein production at a certain time point which cannot reliably be used to estimate protein abundance.[29] Thus, proteomics data better capture changes that occur over time in the tumor. Over the past years, multiple studies showed that proteomics and especially phosphoproteomics (posttranslational regulatory effects) have a significant additional value in cancer research and are especially complementary to transcriptomics.[20–23]

The relatively large observed heterogeneity between GBM tumors is a hallmark of the disease.[5] In this study, this variation was partially excluded by comparing the primary and recurrent GBM tumor samples of individual patients. Pathway analyses on the individual patient level revealed that several statistically significant transcripts and proteins belong to the same pathways. This overlap does not relate to the tumor percentage or any known clinical parameter. Of these pathways, the synaptogenesis signaling pathway/neurotransmitter release cycle is most significant. Transcripts and proteins related to this pathway are found to be upregulated in most of the analyzed patients, 6 of 8. The relationship between synaptogenesis and glioma is reviewed by Gillespie and Monje.[30] A model is introduced in which a bidirectional relationship between neural cells and glioma cells exists. Glioma cells secrete glutamate and synaptogenic factors which results in the release of neuroligin-3 and neurotrophins from neurons that fuel glioma growth and progression.[31] The SNARE complex is part of the synaptogenesis signaling pathway/neurotransmitter release cycle and SNARE proteins have been described in relation to tumorigenesis.[32] In addition, the SNARE complex is involved in autophagy which is connected to TMZ resistance in glioma.[6] Several inhibitors of the SNARE complex are available, including abobotulinumtoxinA, incobotulinumtoxinA, and onabotulinumtoxinA. Inhibition of the SNARE complex with these botulinum toxins showed inhibition of GBM tumor growth in mice.[33] Next to the synaptogenesis pathway, LXR/RXR activation and acute phase signaling pathways are also affected. These pathways overlap in a few patients ($n = 3$) and the direction in which changes occur is also less consistent between patients. LXR relates to cholesterol metabolism which has been connected to glioma survival and has been mentioned as a potential target for therapy.[34] Analysis at the individual patient level clearly helps to identify affected pathways in GBM progression that are shared between patients. However, these pathways are not affected the same way in all patients. For example, patient 6 showed even opposite protein abundance and gene expression changes for the most affected pathways (synaptogenesis signaling, LXR/RXR activation, and GP6 signaling) compared to the other 7 patients.

The size of the phosphoproteomics dataset obtained in this study was limited. This is related to the amount and quality of tissue material available of paired primary and recurrent GBM tumors. In addition, the TMT approach has as a limitation that the input of all samples must be normalized to the sample with the lowest amount. Moreover, each sample was divided over 3 TMT mixes to reduce a potential TMT mix bias. These combined factors had a considerable effect on the protein amount that was available for the phosphopeptide enrichment procedure and resulted in a less rich phosphoproteome dataset. Nevertheless, the obtained phosphoproteomics data show an overlap with previously published data for some phosphosites.[35,36] For instance, phosphorylation of cofilin 1 (CFL1) at the phosphosite S3 was found to be upregulated in GBM.[37] The phosphorylation is regulated by LIM kinases, which in this way deactivate CFL1 and control

actin cytoskeletal dynamics. Perturbations in the normal control of CFL1 activity are known to play a role in cancer metastasis.[35]

The phosphosite S38 of stathmin 1 (STMN1) showed an increase of 0.91 (log2 FC) in the recurrent compared to the primary tumors. The abundance of the protein itself is unchanged indicating that stathmin is at this specific site phosphorylated in a higher degree. For STMN1 activation, the phosphorylation of both S25 and S38 is required.[38] The phosphorylation of STMN1 (S38) is correlated with PI3K pathway activation and is mentioned as a marker of tumor cell proliferation.[36] In addition, a correlation of STMN1 and chemoresistance in cancer has been reported[38] and glioma cell proliferation is known to be promoted by regulating the Akt/p27/stathmin pathway.[39,40] For the STMN1/ERBB4 complex, several inhibitors exist, including afatinib. In a case study of a recurrent GBM patient, treatment with afatinib and TMZ resulted in a significant regression of the disease.[41] In a clinical trial, afatinib was effective in only a limited number of patients indicating that patient selection is needed for this therapy.[42] This suggests that the currently described multiomics approach could potentially be used for patient stratification for this compound.

The development of an adequate universal treatment of GBM patients is, considering the large intertumor heterogeneity, probably unlikely.[43–45] An extra complicating factor for the treatment of GBM is the additional intratumor heterogeneity in space and time of GBM tumors.[46,47] In this study, a multiomics workflow was introduced that uses a longitudinal sampling of primary and recurrent GBM tissues to study tumor progression in individual patients. The advantage of this study design is that samples of the same patient are compared which excludes the interpatient heterogeneity and that intratumor heterogeneity is reduced by focusing on changes (primary vs recurrent) that overlap between at least 3 patients. In addition, complementary data streams are used to identify pathways that change during tumor progression. This approach can be applied on minimal amounts of tissue and the sensitivity of the approach will further increase in the future to obtain more complete data on the proteome and phosphoproteome. In this study, several commonly affected pathways and phosphorylation sites were identified including synaptogenesis, cholesterol metabolism, and phosphorylation of STMN1 (S38). In addition, therapeutics that target these pathways could be identified using the developed pathway analysis module. However, further research and method optimization are required to validate the suggested treatment options. The described workflow can potentially help to further understand the mechanisms related to GBM progression on the individual level and in the future select subgroups of patients for targeted therapy to allow a more patient-tailored treatment.

Supplementary Data

Supplementary data are available at *Neuro-Oncology Advances* online.

Keywords

glioblastoma | multiomics | phosphoproteomics | transcriptomics | tumor progression

Data Availability Statement

The (phospho)proteomics data were deposited to the ProteomeXchange Consortium via the PRIDE partner repository with the dataset identifier PXD017952 and the transcriptomics data to the European Genome-Phenome Archive (EGA) under accession number EGAS00001004345.

Funding

This work has received funding from the Eurostars programme co-funded by Eureka member countries and the European Union Horizon 2020 framework programme (ESTAR1622288, GlioPhos).

Authorship statement. Designed the research: L.D., F.H., E.T., S.L., A.R., and T.L; assembled the patient cohort and generated clinical annotations: L.D., E.T., J.K., and S.L; performed the mass spectrometry experiments: L.D., F.H., and A.R; performed statistical analysis: L.D., N.K., and L.V; developed new pathways visualization tools: D.A.S.H. and J.F; drafted the manuscript: L.D., N.K., A.R., and T.L; read and approved the final version of the manuscript: all authors.

Conflict of interest statement. None declared.

References

1. Rulseh AM, Keller J, Klener J, et al. Long-term survival of patients suffering from glioblastoma multiforme treated with tumor-treating fields. *World J Surg Oncol*. 2012;10:220.
2. McNamara MG, Lwin Z, Jiang H, et al. Conditional probability of survival and post-progression survival in patients with glioblastoma in the temozolomide treatment era. *J Neurooncol*. 2014;117(1):153–160.
3. Nguyen HS, Shabani S, Awad AJ, Kaushal M, Doan N. Molecular markers of therapy-resistant glioblastoma and potential strategy to combat resistance. *Int J Mol Sci*. 2018;19(6):1765.
4. Mandel JJ, Yust-Katz S, Patel AJ, et al. Inability of positive phase II clinical trials of investigational treatments to subsequently predict positive phase III clinical trials in glioblastoma. *Neuro Oncol*. 2017;20(1):113–122.
5. Aum DJ, Kim DH, Beaumont TL, Leuthardt EC, Dunn GP, Kim AH. Molecular and cellular heterogeneity: the hallmark of glioblastoma. *Neurosurg Focus*. 2014;37(6):E11.

6. Yan Y, Xu Z, Dai S, Qian L, Sun L, Gong Z. Targeting autophagy to sensitive glioma to temozolomide treatment. *J Exp Clin Cancer Res.* 2016;35(2):23.
7. Alexander BM, Ba S, Berger MS, et al.; GBM AGILE Network. Adaptive global innovative learning environment for glioblastoma: GBM AGILE. *Clin Cancer Res.* 2018;24(4):737–743.
8. Azuaje F, Tiemann K, Niclou SP. Therapeutic control and resistance of the EGFR-driven signaling network in glioblastoma. *Cell Commun Signal.* 2015;13:23.
9. Ma Y, Tang N, Thompson RC, et al. InsR/IGF1R pathway mediates resistance to EGFR inhibitors in glioblastoma. *Clin Cancer Res.* 2016;22(7):1767–1776.
10. Ueno H, Tomiyama A, Yamaguchi H, et al. Augmentation of invadopodia formation in temozolomide-resistant or adopted glioma is regulated by c-Jun terminal kinase-paxillin axis. *Biochem Biophys Res Commun.* 2015;468(1–2):240–247.
11. Garralda E, Dienstmann R, Piris-Giménez A, Braña I, Rodon J, Tabernero J. New clinical trial designs in the era of precision medicine. *Mol Oncol.* 2019;13(3):549–557.
12. Wang Q, Hu B, Hu X, et al. Tumor evolution of glioma-intrinsic gene expression subtypes associates with immunological changes in the microenvironment. *Cancer Cell.* 2017;32(1):42–56.e46.
13. Verhaak RG, Hoadley KA, Purdom E, et al.; Cancer Genome Atlas Research Network. Integrated genomic analysis identifies clinically relevant subtypes of glioblastoma characterized by abnormalities in PDGFRA, IDH1, EGFR, and NF1. *Cancer Cell.* 2010;17(1):98–110.
14. van den Bent MJ, Gao Y, Kerkhof M, et al. Changes in the EGFR amplification and EGFRvIII expression between paired primary and recurrent glioblastomas. *Neuro Oncol.* 2015;17(7):935–941.
15. Draaisma K, Chatzipli A, Taphoorn M, et al. Molecular evolution of IDH wild-type glioblastomas treated with standard of care affects survival and design of precision medicine trials: a report from the EORTC 1542 study. *J Clin Oncol.* 2020;38(1):81–99.
16. Consortium G. Glioma through the looking GLASS: molecular evolution of diffuse gliomas and the glioma longitudinal analysis consortium. *Neuro Oncol.* 2018;20(7):873–884.
17. Sung J, Wang Y, Chandrasekaran S, Witten DM, Price ND. Molecular signatures from omics data: from chaos to consensus. *Biotechnol J.* 2012;7(8):946–957.
18. Papaioannou MD, Djuric U, Kao J, et al. Proteomic analysis of meningiomas reveals clinically-distinct molecular patterns. *Neuro Oncol.* 2011;21(8):1028–1038.
19. Mathé E, Hays JL, Stover DG, Chen JL. The omics revolution continues: the maturation of high-throughput biological data sources. *Yearb Med Inform.* 2018;27(1):211–222.
20. Boja ES, Rodriguez H. Proteogenomic convergence for understanding cancer pathways and networks. *Clin Proteomics.* 2014;11(1):22.
21. Mertins P, Mani DR, Ruggles KV, et al.; NCI CPTAC. Proteogenomics connects somatic mutations to signalling in breast cancer. *Nature.* 2016;534(7605):55–62.
22. Vogel C, Marcotte EM. Insights into the regulation of protein abundance from proteomic and transcriptomic analyses. *Nat Rev Genet.* 2012;13(4):227–232.
23. Doll S, Gnad F, Mann M. The case for proteomics and phosphoproteomics in personalized cancer medicine. *Proteomics Clin Appl.* 2019;13(2):e1800113.
24. Ressa A, Bosdriesz E, de Ligt J, et al. A system-wide approach to monitor responses to synergistic BRAF and EGFR inhibition in colorectal cancer cells. *Mol Cell Proteomics.* 2018;17(10):1892–1908.
25. Stupp R, Mason WP, van den Bent MJ, et al.; European Organisation for Research and Treatment of Cancer Brain Tumor and Radiotherapy Groups; National Cancer Institute of Canada Clinical Trials Group. Radiotherapy plus concomitant and adjuvant temozolomide for glioblastoma. *N Engl J Med.* 2005;352(10):987–996.
26. Gierlinski M, Gastaldello F, Cole C, Barton GJ. Proteus: an R package for downstream analysis of MaxQuant output. *bioRxiv.* 2018:416511.
27. Huse JT, Phillips HS, Brennan CW. Molecular subclassification of diffuse gliomas: seeing order in the chaos. *Glia.* 2011;59(8):1190–1199.
28. Phillips HS, Kharbanda S, Chen R, et al. Molecular subclasses of high-grade glioma predict prognosis, delineate a pattern of disease progression, and resemble stages in neurogenesis. *Cancer Cell.* 2006;9(3):157–173.
29. Hegde PS, White IR, Debouck C. Interplay of transcriptomics and proteomics. *Curr Opin Biotechnol.* 2003;14(6):647–651.
30. Gillespie S, Monje M. An active role for neurons in glioma progression: making sense of Scherer's structures. *Neuro Oncol.* 2018;20(10):1292–1299.
31. John Lin CC, Yu K, Hatcher A, et al. Identification of diverse astrocyte populations and their malignant analogs. *Nat Neurosci.* 2017;20(3):396–405.
32. Meng J, Wang J. Role of SNARE proteins in tumourigenesis and their potential as targets for novel anti-cancer therapeutics. *Biochim Biophys Acta.* 2015;1856(1):1–12.
33. Ulloa F, Gonzàlez-Juncà A, Meffre D, et al. Blockade of the SNARE protein syntaxin 1 inhibits glioblastoma tumor growth. *PLoS One.* 2015;10(3):e0119707.
34. Ahmad F, Sun Q, Patel D, Stommel JM. Cholesterol metabolism: a potential therapeutic target in glioblastoma. *Cancers.* 2019;11(2):146.
35. Mizuno K. Signaling mechanisms and functional roles of cofilin phosphorylation and dephosphorylation. *Cell Signal.* 2013;25(2):457–469.
36. Wik E, Birkeland E, Trovik J, et al. High phospho-Stathmin (Serine38) expression identifies aggressive endometrial cancer and suggests an association with PI3K inhibition. *Clin Cancer Res.* 2013;19(9):2331–2341.
37. Park JB, Agnihotri S, Golbourn B, et al. Transcriptional profiling of GBM invasion genes identifies effective inhibitors of the LIM kinase-Cofilin pathway. *Oncotarget.* 2014;5(19):9382–9395.
38. Biaoxue R, Xiguang C, Hua L, Shuanying Y. Stathmin-dependent molecular targeting therapy for malignant tumor: the latest 5 years' discoveries and developments. *J Transl Med.* 2016;14(1):279.
39. Xie M, Ji Z, Bao Y, et al. PHAP1 promotes glioma cell proliferation by regulating the Akt/p27/stathmin pathway. *J Cell Mol Med.* 2018;22(7):3595–3604.
40. Marie SK, Oba-Shinjo SM, da Silva R, et al. Stathmin involvement in the maternal embryonic leucine zipper kinase pathway in glioblastoma. *Proteome Sci.* 2016;14:6.
41. Alshami J, Guiot MC, Owen S, et al. Afatinib, an irreversible ErbB family blocker, with protracted temozolomide in recurrent glioblastoma: a case report. *Oncotarget.* 2015;6(32):34030–34037.
42. Reardon DA, Nabors LB, Mason WP, et al.; BI 1200 36 Trial Group and the Canadian Brain Tumour Consortium. Phase I/randomized phase II study of afatinib, an irreversible ErbB family blocker, with or without protracted temozolomide in adults with recurrent glioblastoma. *Neuro Oncol.* 2015;17(3):430–439.
43. Dirkse A, Golebiewska A, Buder T, et al. Stem cell-associated heterogeneity in glioblastoma results from intrinsic tumor plasticity shaped by the microenvironment. *Nat Commun.* 2019;10(1):1787.
44. Friedmann-Morvinski D. Glioblastoma heterogeneity and cancer cell plasticity. *Crit Rev Oncog.* 2014;19(5):327–336.
45. Niclou SP. Gauging heterogeneity in primary versus recurrent glioblastoma. *Neuro Oncol.* 2015;17(7):907–909.
46. Jacob F, Salinas RD, Zhang DY, et al. A patient-derived glioblastoma organoid model and biobank recapitulates inter- and intra-tumoral heterogeneity. *Cell.* 2020;180(1):188–204.e22.
47. Sottoriva A, Spiteri I, Piccirillo SG, et al. Intratumor heterogeneity in human glioblastoma reflects cancer evolutionary dynamics. *Proc Natl Acad Sci U S A.* 2013;110(10):4009–4014.